scientific reports

Check for updates

OPEN

Remodeling of the cardiac striatin interactome and its dynamics in the diabetic heart

Stephanie Chacar[1,11], Wael Abdrabou[2,11], Cynthia Al Hageh[3], Liaqat Ali[4], Thenmozhi Venkatachalam[5], Pierre Zalloua[3,6], M.-Saadeh Suleiman[7], Frank Christopher Howarth[8], Ali A. Khraibi[9] & Moni Nader[1,10]✉

Diabetic cardiomyopathy (DbCM) is a silent and complex condition involving numerous signaling pathways that impair cardiomyocyte metabolism and cardiac performance. Striatin (STRN) is a multifaceted protein that binds metabolic proteins, yet its role in diabetic heart remains unexplored. Here we characterized the cardiac STRN interactome by performing immunoprecipitation on left ventricle (LV) proteins from control and diabetic hearts (rats treated with streptozotocin for 24 weeks) to dissect its derivative protein complex. Diabetic rats exhibited pathological heart remodeling characterized by increased heart weight/body weight ratio, elevated levels of Atrial Natriuretic Factor (ANF), and altered expression of alpha and beta-myosin heavy chain isoforms. Notably, STRN expression mirrored that of the remodeling marker ANF across all cardiac chambers. Proteomic analysis yielded 247 proteins interacting with STRN exclusively in diabetic LV, 94 in both control and diabetic LV, and 11 only in control LV. STRN retained a higher interaction with some STRN interacting phosphatase and kinase complex (STRIPAK) proteins (i.e. protein phosphatase 2A (PP2A), and sarcolemmal associated membrane protein (SLMAP)) in diabetic LV, indicating a preserved role of this signalosome in diabetic settings. Functional enrichment and gene ontology revealed that the STRN interactome in diabetic LV carried signalosomes related to cardiac contractility, endoplasmic reticulum stress, mitochondrial function, and apoptotic processes. Western blot experiments confirmed the interaction between STRN and SLMAP in both control and diabetic heart. These data suggest a pivotal role for the STRN signalosome in cardiometabolic disorders, potentially paving the way for novel therapeutic management of DbCM. Targeting the STRN interactome in DbCM, mainly the first-line interactors SLMAP, PP2A, and Cav-1 may offer hope for patients with diabetes-induced cardiac injuries.

Keywords Diabetic cardiomyopathy, Striatin interactome, Diabetes, Signalosomes, Metabolic Disease

Diabetic cardiomyopathy (DbCM) is a silent manifestation in patients with uncontrolled hyperglycemia characterized by systolic/diastolic dysfunction without the presence of known risk factors for cardiovascular diseases[1]. Given the current worldwide projections for diabetes in 2050, there is a serious concern for the spread of cardiac complications due to the absence of a cure for DbCM[2]. Our poor understanding of the complex etiology of DbCM, particularly the role of metabolic signalosomes (protein networks regulating signaling pathways) implicated in the onset of the pathological cascades driving the diabetic heart into failure, limits the progress in developing targeted therapeutic strategies[3].

[1]Department of Medical Sciences, College of Medicine and Health Sciences, Khalifa University of Science and Technology, Abu Dhabi, United Arab Emirates. [2]Program in Biology, Division of Science and Mathematics, New York University Abu Dhabi, Abu Dhabi, United Arab Emirates. [3]Department of Public Health and Epidemiology, College of Medicine and Health Sciences, Khalifa University of Science and Technology, Abu Dhabi, United Arab Emirates. [4]Core Technology Platforms, New York University Abu Dhabi, Abu Dhabi, United Arab Emirates. [5]Department of Biological Sciences, College of Medicine and Health Sciences, Khalifa University of Science and Technology, Abu Dhabi, United Arab Emirates. [6]Harvard T.H. Chan School of Public Health, Boston, MA, USA. [7]Bristol Medical School (THS), University of Bristol, Bristol, UK. [8]Department of Physiology, College of Medicine and Health Sciences, United Arab Emirates University, Al Ain, United Arab Emirates. [9]Department of Biomedical Engineering and Biotechnology, College of Medicine and Health Sciences, Khalifa University of Science and Technology, Abu Dhabi, United Arab Emirates. [10]Department of Physiological Sciences, College of Medicine, Alfaisal University, Riyadh, Kingdom of Saudi Arabia. [11]Stephanie Chacar and Wael Abdrabou contributed equally to this work. ✉email: mnader@alfaisal.edu

Striatin (STRN) is a scaffold protein that was identified as a regulatory subunit of the trimeric holoenzyme protein phosphatase 2 A (PP2A)[4]. It possesses binding capabilities to proteins implicated in various cellular functions[5] some of which are involved in cardiac remodeling and metabolic disorders, particularly diabetes. While the literature extensively highlights the role of STRN in various cellular functions using mainly cultured cell lines (more specifically cancer cells)[6]; the role of STRN in the diabetic heart is not yet elucidated. Interestingly, studies showed that the protein STRN contains binding domains for important molecules that are implicated in diabetes and are central for cardiac function/dysfunction. These include calmodulin (CaM)[7], PP2A[8], caveolin (Cav)[9], and the sarcolemmal associated membrane protein (SLMAP)[10] among others (Fig. 3). Several of these proteins have been implicated in the pathogenesis of DbCM. For example, Galbo et al. reported that PP2A plays a primordial role in the development of insulin resistance and glucose metabolism, while others characterized a direct role of PP2A in DbCM and its derivative injuries to the myocardium[11–14]. Similarly, caveolins have been shown to regulate signalosomes involved in DbCM (i.e.NF-κB and the mitochondrial complex I) and its derived myocardial injuries[15,16]. Additionally, the membrane protein SLMAP, which is central in organizing cardiomyocyte membranes and cardiac function, has also been implicated in diabetic complications[17]. All together, these studies highlight an important role for the STRN interactome (Network of STRN-interacting proteins) in diabetes.

In the same vein, reduction in both calcium (Ca^{2+}) transients and contraction has been reported in the diabetic cardiomyocyte, thus leading to systolic and diastolic dysfunction[18]. We previously reported that STRN localizes to hot spots in cardiomyocytes, more precisely the caveola and t-tubules, and that it interacts with signalosomes implicated in cardiac function to relay biological signals from the sarcolemma to the internal environment of cardiomyocytes[17]. We also showed that, in cardiomyocytes, cardiac STRN interacts with CaM and Caveolin-3 in a Ca^{2+}- sensitive manner to control their contraction[19]. Nonetheless, there are few studies highlighting the implication of STRN in cardiac function with focus on arrhythmogenic right ventricular tachycardia[20], hypertension[21,22], cardiac hypertrophy (Induced by angiotensin II), together with a role for STRN in regulating sodium currents in iPSC-derived cardiomyocytes[23,24].

In view of its role in cardiac function as well as its interaction with metabolic proteins that are involved in diabetes, we sought to investigate the cardiac protein network of STRN in remodeled diabetic hearts. Therefore, we assessed the expression of STRN and Atrial Natriuretic Factor (ANF) in the four chambers of diabetic heart to link its expression with pathological cardiac remodeling. We also immunoprecipitated STRN from the remodeled LVs of diabetic rats at chronic stage of diabetes (24 weeks post-streptozotocin), and we dissected the diabetic STRN interactome by tandem mass tagging (TMT) mass spectrometry. We found that in diabetic hearts, cardiac STRN expression paralleled that of the remodeling maker ANF in all heart chambers. We also found that STRN interacts with proteins mainly involved in cardiac contractility, endoplasmic reticulum stress, mitochondrial function, and apoptotic processes. Moreover, several key proteins of the STRIPAK complex (i.e. PP2A, Cav-1, and SLMAP) showed enhanced interaction with STRN in diabetic hearts which highlights a functional signature of STRN in this signaling complex in DbCM.

Material and methods

Experimental model of streptozotocin-induced diabetes

The present study was approved by the Animal Research Oversight Committee (AROC) of Khalifa University (KU) of Science and Technology and by the College of Medicine & Health Sciences Animal Ethics Committee of United Arab Emirates University (UAEU). All methods were performed in accordance with ARRIVE guidelines and the relevant guidelines and regulations of the AROC. The animals were housed at the animal care facility of UAEU in a temperature (22 ± 2 °C) and humidity (40–60%) controlled area with a 12/12 h light/dark cycle. They were fed ordinary rodent chow and were acclimatized at least 1 week under these conditions before the start of the study. Eight male Wistar rats weighting 245–300 g were randomly divided into a diabetic group (n = 4) where rats were injected intraperitoneally with streptozotocin (STZ) (S0130, Sigma-Aldrich) dissolved in citrate buffer (60 mg/kg body weight), and a control group (n = 4) injected with citrate buffer alone. Experiments were performed 24 weeks after STZ treatment. Two-days after STZ injection, and on the day of heart extraction, blood glucose was estimated using glucose test strips for control and STZ groups confirming sustained hyperglycemia in our animal model (Fig. 1). The body weight of the experimental rats was measured, animals were sacrificed by decapitation using a guillotine then the hearts were removed, weighed, perfused with ice-cold phosphaste-buffered saline (PBS), and stored at − 80 °C for further processing.

Protein extraction and Western blot

Cardiac LVs were minced with fine scissors and homogenized in ice-cold lysis radioimmunoprecipitation assay buffer (RIPA buffer, Cat. No. R0278, Sigma–Aldrich) supplemented with complete protease inhibitor cocktail (Cat. No. 11836145001, Roche) using an electric TissueRuptor (Qiagen), on ice. Samples were kept on ice for 30 min for maximal yield of proteins. The homogenate was cleared by centrifugation (10,000*g*, 5 min, 4 °C) and the supernatant was collected. Protein concentration was determined using the Pierce BCA protein assay kit (Cat. No. 23225, Thermo Fisher Scientific) according to the manufacturer's protocol. 20 µg of proteins were size fractionated on a 10% polyacrylamide gel, and transferred on a PVDF membrane. Blots were probed with antibodies for the following proteins: α-MHC (Mouse cardiac alpha-myosin heavy chain antibody, 1:1000, ab50967, Abcam), β-MHC (Mouse, beta-myosin heavy chain, 1:1000, ab11083, Abcam) and GAPDH (anti-glyceraldehyde 3-phosphate dehydrogenase mouse antibody, 1:1000, Cat#5174, CST) for loading control. Secondary antibody (anti-mouse) linked to horse radish peroxidase (HRP) was used as appropriate, and the protein bands were revealed with ECL chemiluminescent substrate (Bio-Rad Laboratories, Inc.) using the Azure biosystems 400 imaging system. Densitometry analysis of the protein bands was determined using ImageJ software (NIH).

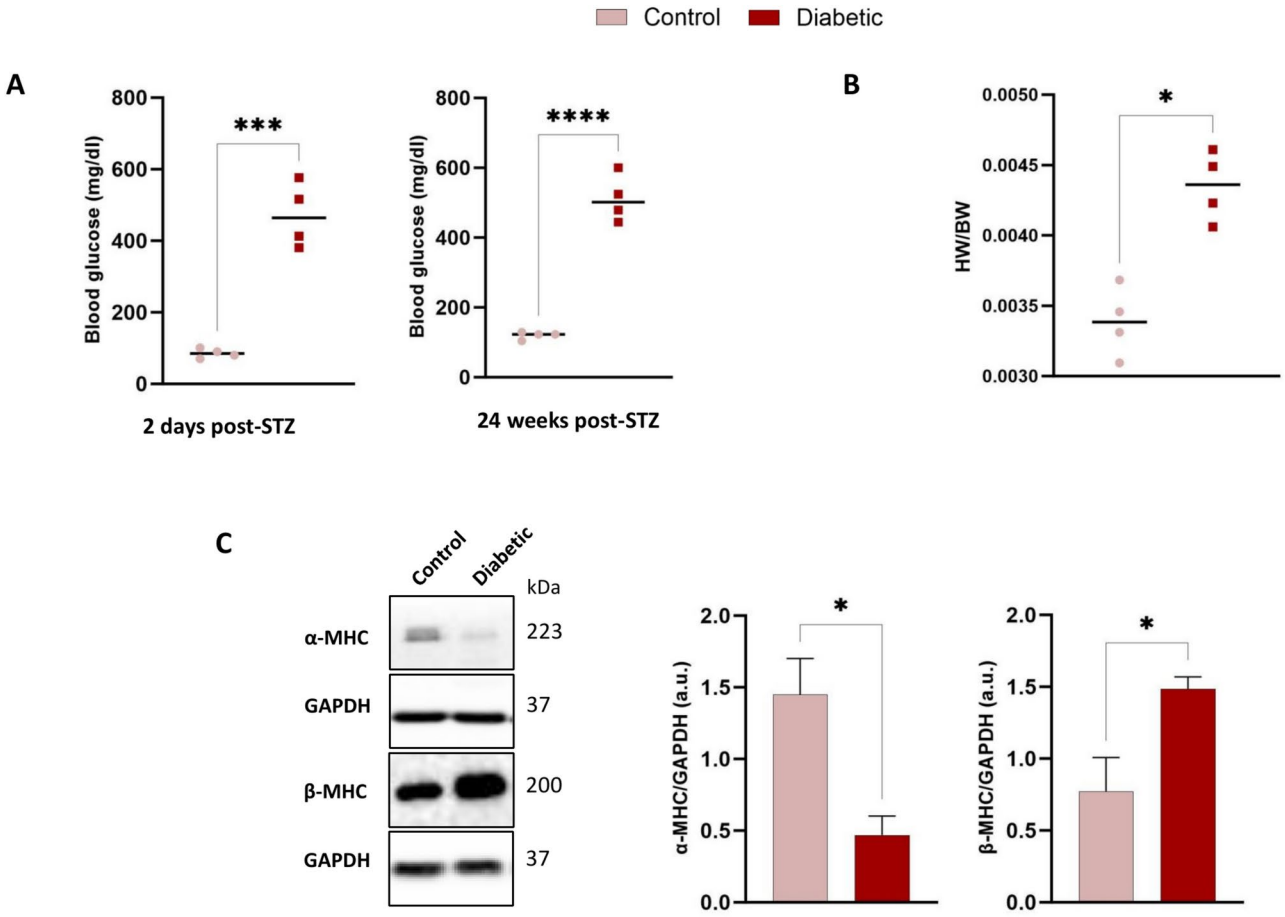

Fig. 1. Blood glucose level and cardiac remodeling in STZ-treated rats. (**A**) Blood glucose level 2 days and 24 weeks after STZ injection (Control n = 4, Diabetic n = 4) (**B**) HW/BW after 24 weeks of STZ treatment. (**C**). Representative western blot bands and histogram analysis for α and β-MHC in control and diabetic rat hearts at 24 weeks post-STZ treatment, normalized to GAPDH (in arbitrary units, a.u.). Values represent mean ± SEM (n = 4 samples for each protein and condition). *$p < 0.05$, **$p < 0.01$, ****$p < 0.0001$, using Students' t-test. Control data are shown in light red, and diabetic data are shown in dark red across all jitter plots and histograms.

Gene	Forward primer (5′–3′)	Reverse primer (3′–5′)
rANF	TTCTCCATCACCAAGGGCTT	GACCTCATCTTCTACCGGCA
rSTRN	GCTTGTTGTCCTGTTCAGCA	CCTTGCTGAACGATGCTACC
rGAPDH	GTATGACTCTACCCACGGCA	GCCAGTAGACTCCACGACAT

Table 1. List of primers used in this study.

RNA extraction and quantitative real time PCR

Left ventricle tissues were homogenized and total RNA was extracted using Qiazol Lysis reagent (Qiagen, Germany) following manufacturer's instruction. The extracted RNA was quantified using nanodrop (Invitrogen, USA), and 1 µg of RNA was used to generate complementary DNA (cDNA) using high-capacity cDNA synthesis kit (Thermo Scientific). RT–qPCR was performed using HOT FIREPol® EvaGreen® qPCR Mix Plus (Solis Biodine, Estonia) on Bio-Rad CFX96 real-time PCR system (Bio-Rad, USA). Relative quantification was expressed as $2^{-\Delta\Delta Ct}$, where $\Delta\Delta Ct$ is the difference between the ΔCt values of the control and the diabetes samples analyzed in triplicates. GAPDH gene was used as endogenous control. Table 1 details the primers used in the RT–qPCR assays.

Immunoprecipitation

A total of 500 µg of LV lysates from either control (n = 4) or diabetic (n = 4) rats were incubated with 2.5 µg of STRN antibody (BD #610838), and 500 µg from the same lysates were also incubated with 2.5 µg of mouse IgG (mIgG) antibody (CST #5415) as a negative control. Samples were maintained overnight at 4 °C on a

rotator. Next day, for each sample, a volume of 50 µl of Dynabeads Protein G Immunoprecipitation (IP) kit (Invitrogen Catalog number: 10007D) was prepared on an Invitrogen™ DynaMag™-2 Magnet set-up, according to the manufacturer's protocol. The dynabeads were subsequently resuspended in 200 µl of washing + antibody binding buffer, and added to the lysate + antibody solution (STRN or mIgG). The mixture underwent a 3-h rotation at 4 °C on a sample mixer. Following IP, three washes were performed using 200 µl of washing buffer, and the protein complex was eluted by boiling for 5 min. Proteins were separated on a 10% polyacrylamide gel as detailed in the Western blot section and the blots were probed with anti-STRN antibody to validate this assay, before interrogating the STRN protein complex using Liquid Chromatography/Mass Spectrometry (LC/MS) proteomics. The same steps were performed and the protein complex was labelled with TMT for the quantitative proteomics analysis as detailed in the next sections.

To validate the STRN-SLMAP interaction in our animal model, IP assay was performed in which 500 µg of rat LV lysates (Control and diabetic) were incubated with 2.5 µg of SLMAP antibody (Abnova #677784), and 500 µg from the same preparations were also incubated with 2.5 µg of mouse IgG (mIgG) antibody (CST #5415) as a negative control. Similar steps were followed as detailed in the previous paragraph. The SLMAP complexed proteins were dissociated by boiling 5 min and the denatured proteins were loaded on a polyacrylamide gel for Western blot analysis. The membrane was blotted with anti-SLMAP and anti-STRN and was revealed with protein A/G-HRP to avoid non-specific bands pertaining to the IgG fragments (~ 25 and 50 kDa). This assay was used to validate the STRN/SLMAP interaction identified by proteomic profiling.

Preparation of protein digests and high pH reversed-phase fractionation of labelled peptides

Immuno-isolated samples were reduced, S-alkylated and digested from the beads (1.25 µg trypsin/lys-C, 37 °C, overnight). The peptide digests were TMT labelled then pooled and desalted using a SepPak cartridge according to the manufacturer's instructions (Waters). The eluted peptides from the cartridge were fractionated by high pH reversed-phase chromatography system (Ultimate 3000 HPLC, Thermo Fisher Scientific). In brief, the peptide digests were loaded onto a C18 Column (XBridge BEH, 130 Å, 3.5 µm, 2.1 mm × 150 mm, Waters) in buffer A and eluted with an increasing gradient of buffer B (20 mM Ammonium hydroxide in acetonitrile, pH 10) from 0 to 95% over 60 min. The resulting fractions (8 in total) were dried and resuspended in 1% formic acid prior to online liquid chromatography tandem mass spectrometry (LC–MS/MS, Orbitrap Fusion Lumos, Thermo Scientific).

Liquid chromatography tandem mass spectrometry

The LC–MS/MS was performed on a fully automated Ultimate 3000 nano-LC system in line with an Orbitrap Fusion Lumos mass spectrometer (Thermo Scientific). Mobile phases consisted of 0.1% formic acid for solvent A and 0.1% formic acid in 80% acetonitrile for solvent B. In brief, peptides in solvent A were injected onto a C18 nano-trap column (Acclaim PepMap, Thermo Scientific). After washing with 0.5% (vol/vol) acetonitrile 0.1% (vol/vol) formic acid, peptides were resolved on a C18 analytical column (Acclaim PepMap, 250 mm × 75 µm, Thermo Scientific) over a 150 min linear gradient. The gradient was set as follows: 1–6% B for 1 min, 6–15% B for 58 min, 15–32% B for 58 min and 32–40% B for 5 min. A 6-min wash at 90% B was used to prevent carryover and 10-min equilibration at 1% B completed the gradient. A constant flow rate of 300 nl min^{-1} was used. Peptides were ionized by nano-electrospray ionization at 2.0 kV using a stainless-steel emitter with an internal diameter of 30 µm (Thermo Scientific) and a capillary temperature of 300 °C.

The spectra were acquired with an Orbitrap Fusion Lumos system operated in data-dependent acquisition mode using an SPS-MS3 workflow. FTMS1 (Fourier Transform Mass Spectrometry) spectra were collected at a resolution of 120,000, an automatic gain control (AGC) target of 200,000 and a max injection time of 50 ms. Precursors were filtered with an intensity threshold of 5000 according to charge state (to include charge states 2–7) and with monoisotopic peak determination set to Peptide. Previously interrogated precursors were excluded using a dynamic window (60 s ± 10 ppm). The MS2 precursors were isolated with a quadrupole isolation window of 0.7 m/*z*. ITMS2 (Ion Trap Mass Spectrometry) spectra were collected with an AGC target of 10,000, max injection time of 70 ms and CID collision energy of 35%.

For FTMS3 analysis, the Orbitrap was operated at a resolution of 50,000, an AGC target of 50,000 and a max injection time of 105 ms. Precursors were fragmented by high energy collision dissociation (HCD) at a normalized collision energy of 60% to ensure maximal TMT reporter ion yield. Synchronous precursor selection (SPS) was enabled to include up to 10 MS2 fragment ions in the FTMS3 scan.

Mass spectrometry data curation and statistical analysis

The mass spectrometry data were searched against the rat Uniprot database protein groupings determined by PD2.4 refined using a custom script to select the best annotated master proteins. Peptide matches to multiple proteins were resolved by referring to the list of master proteins determined during total protein analysis. Raw IP values representing the abundance of each protein compound were subject to log transformation (log2). Only proteins with values in all four samples representing each condition were considered for downstream analysis. Unsupervised and supervised statistical analyses were performed on IP data that passed the quality control step. The analysis was performed using MetaboAnalyst v6.0[25]. The data was curated by normalizing all the peptides abundance from each sample to the abundances of STRN peptide in the same samples. The abundance of proteins for the STRN IP for each rat was divided by the abundance of proteins of the corresponding IgG control. The derived values were log2 transformed and the fold change (FC) and *p* values were determined to carry on statistical tests and plot the graphs as detailed in the corresponding figure legends of the results section[5].

Pathway enrichment and network analyses of immunoprecipitation hits

Proteins interacting with STRN in diabetic LVs were searched against *Rattus norvegicus* UniProt proteome database using its ID mapping tool (https://www.uniprot.org/proteomes/UP000002494). Proteins showing significantly differential binding to STRN in diabetic LVs were subsequently subjected to protein–protein interaction (PPI) analysis using String analysis tools (www.string-db.org) to identify all implicated molecular functions and biological processes in this network of proteins. K-means clustering was applied on the whole network and false discovery rate (FDR) was used to infer statistical significance for each enriched term and process. *p* Values were corrected for multiple testing within each term using the Benjamini–Hochberg procedure. Identified clusters of proteins in our network were searched against the curated *Rattus norvegicus* proteins as background, and were annotated and assigned to all particular biological terms. The strength of enrichment of a particular term was determined by calculating the ratio between (i) the number of proteins in our network that are annotated with a term and (ii) the number of proteins that are expected to be annotated with this term in a random network of the same size, expressed as Log10(observed/expected).

Statistical analyses

Statistical analyses were run using graphpad prism (version 10.0). The results were expressed as mean ± SEM of n samples. Unpaired t-test was employed and the results were considered statistically significant at $p < 0.05$.

Results

Pathological cardiac remodeling in STZ-treated rats

STZ was used as a single injection in rats to induce type 1 diabetes (T1D). Blood glucose levels of all rats were measured 2 days post-STZ injection, and on the day when the rats were culled (24 weeks post-STZ). As shown in Fig. 1A, the STZ-induced diabetic rats exhibited a fivefold increase in blood glucose levels at the two different time points (2 days and 24 weeks post-STZ) compared to controls, indicating sustained hyperglycemia in our animal model. The increased heart weight/body weight (HW/BW) ratio in the diabetic rats indicates cardiac hypertrophy (Fig. 1B). This remodeling was supported by the increased expression of ANF and β-MHC isoform, paralleled with a decline in the expression of the α-MHC isoform (Fig. 1C and 2), thus indicating a pathological remodeling of these hearts[26].

STRN expression parallels that of ANF in cardiac chambers at 24 weeks post-STZ

We investigated the expression of STRN gene in the four chambers of diabetic heart, along with the marker of cardiac remodelling, ANF. Real time PCR data showed that the expression of STRN mRNA mirrored the expression of ANF. Specifically, both STRN and ANF showed significant increase in the right atrium, left atrium, and left ventricle, whereas the variations in their expression in the right ventricle were not statistically significant (Fig. 2). Together, these data showed a correlated expression of STRN with that of the cardiac remodeling genes in the diabetic heart, thus implicating STRN in DbCM.

Structural features and domain composition of STRN

To gain insight into the structural organization of STRN, we utilized AlphaFold to generate a predicted 3D model of the protein. This structure, supported by sequence analysis, revealed distinct domains (caveolin binding domain, coiled-coil motif, PP2A-A and C, STRN interactive proteins STRIP1 and STRIP2, SLMAP and calmodulin binding domain with WD40 repeat at the C-terminal) that likely contribute to STRN's role in cellular processes (Fig. 3).

Characterization of the cardiac STRN protein complex in control and diabetic left ventricle

STRING analysis illustrated in Fig. 4A showed a network of proteins interacting with STRN; however, this network has not been investigated in the heart. To evaluate the protein network that interacts with cardiac STRN and its dynamics in diabetic heart, we performed an IP of STRN on solubilized protein extracts from both control and diabetic rat LV, with a specific monoclonal antibody for STRN. Immunoblotting revealed that STRN was successfully immunoprecipitated in both control and diabetic LVs denoted by a single lucid band that corresponded to the same STRN band that is detected in the input, but was absent in the control mouse IgG Lane (Fig. 4B). We further performed TMT labelled quantitative analysis on the immunoprecipitated proteins using the STRN antibody. Proteins interacting with STRN are presented in Fig. 4C as three quadrants (Control LV, diabetic LV, and common to both control and diabetic conditions). The identified proteins were searched against the curated Rattus norvegicus UniProt proteome database (https://www.uniprot.org/proteomes/UP000002494) using UniProt ID mapping tool to identify their corresponding gene/protein IDs.

Interestingly, we identified 247 proteins interacting with STRN exclusively in diabetic LV, highlighting the significant alterations in protein interactions under diabetic conditions. Structural proteins mainly included Myh9, Myh7, Tuba4a, actin, Actc1. Mitochondrial proteins such as Vdac1, Vdac2, Slc25a11 and Mrpl47 were identified. The metabolic enzymes that were identified included Nnt, Sdha, Pfkm, Dlat. It is worth noting that the following proteins PP2A-A subunit, PP2A-B subunit, SLMAP, and Cav-1 (encoded by ppp2r1a, ppp2r2a, slmap, and cav-1 genes, respectively) showed high interaction with STRN in the diabetic LVs than controls suggesting a role for this complex in diabetes-induced cardiac remodeling.

In our analysis of PPI with STRN, 94 proteins were identified in both control and diabetic LV. Metabolic enzymes involved in energy metabolism included Pkm and Tkt. Heat shock proteins crucial for protein folding and stress responses such as Hsp90ab1, Hspa8, Hsp90aa1, and Hspa4 were prevalent. Various cytoskeletal and structural proteins such as keratins (KRT6A, KRT6B, KRT10 etc.) and actin-related proteins (Actr3, Arpc3) were also precipitated with STRN, showing interactions with components essential for maintaining cellular architecture. The presence of translation and elongation factors (Eef2, Eef1g, Eif3a etc.) was also noted suggesting

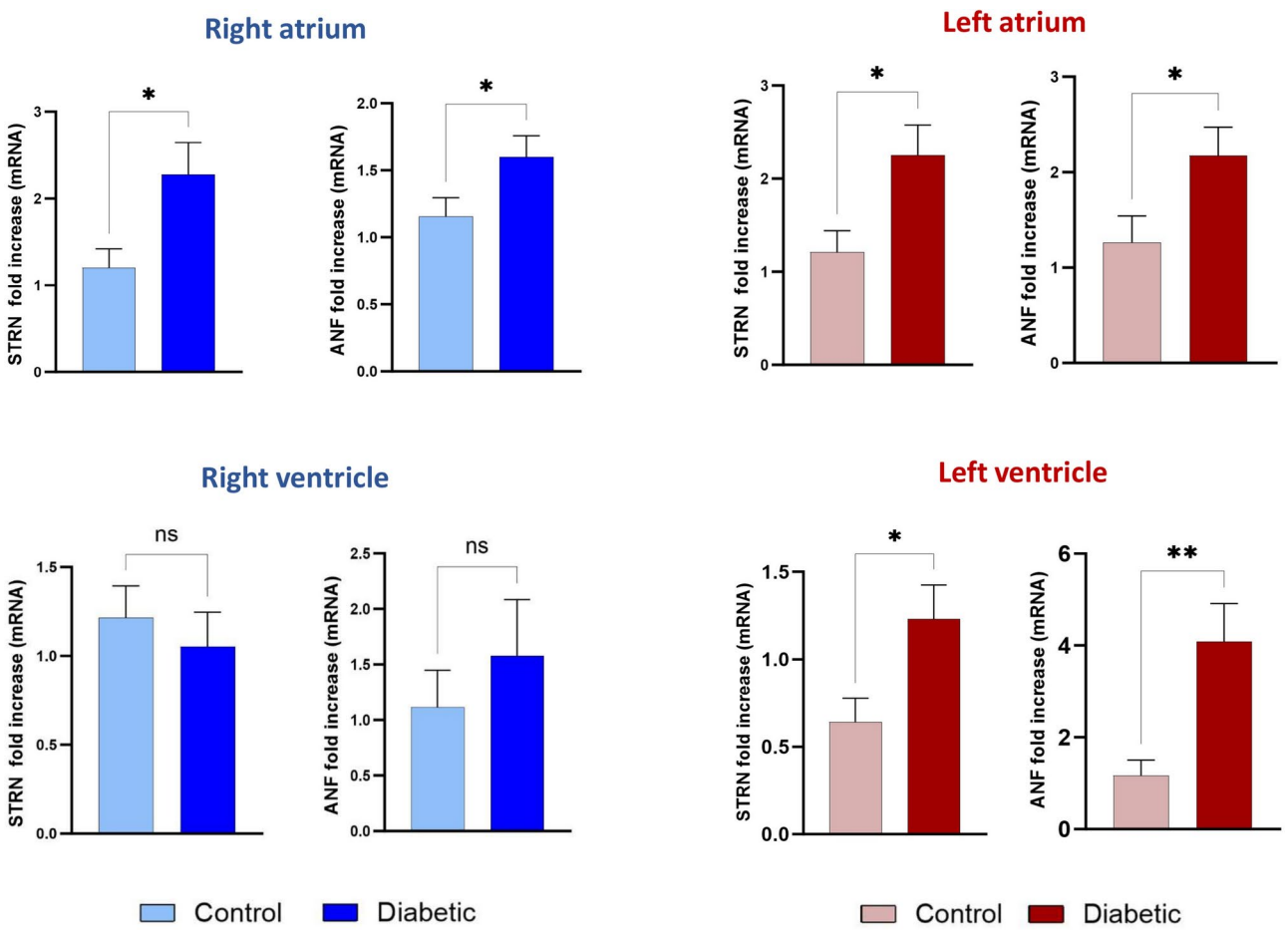

Fig. 2. Expression of STRN and ANF in the heart chambers of rats at 24 weeks after STZ treatment. Histograms of the mRNA expression of STRN and ANF presented as log fold change relative to the control groups, post normalization to the housekeeping gene GAPDH. Values represent mean ± SEM (n = 9–12 samples for each marker and condition) $*p < 0.05$, $**p < 0.01$, ns: not significant, using Student's t-test.

Strn

Information
Striatin; Binds calmodulin in a calcium dependent manner. May function as scaffolding or signaling protein; Belongs to the WD repeat striatin family

Identifier: ENSRNOP00000006527, Strn
Organism: Rattus novergicus

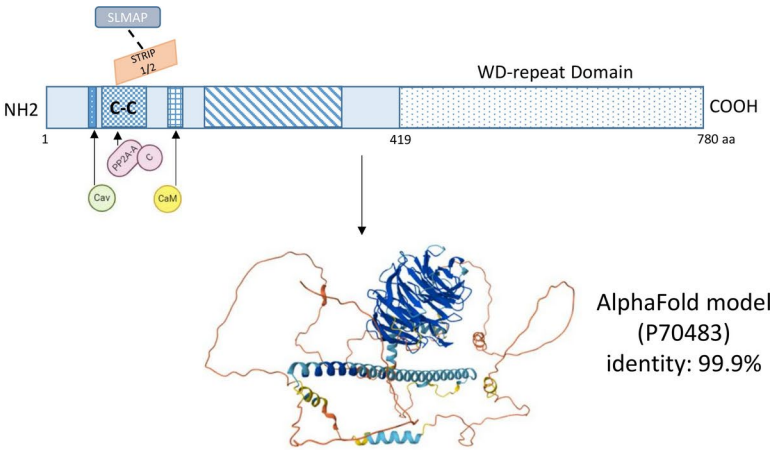

Fig. 3. STRN protein structure. STRN sequence and structure predicted by AlphaFold[57]. Domain structure of STRN from N to C terminus adopted from[8,58]: Cav: caveolin-binding domain, C–C: coiled–coil domain, PP2A: Protein Phosphatase 2a, STRIP: STRN interactive proteins, SLMAP: sarcolemmal membrane-associated protein, CaM: calmodulin binding domain and WD-repeats.

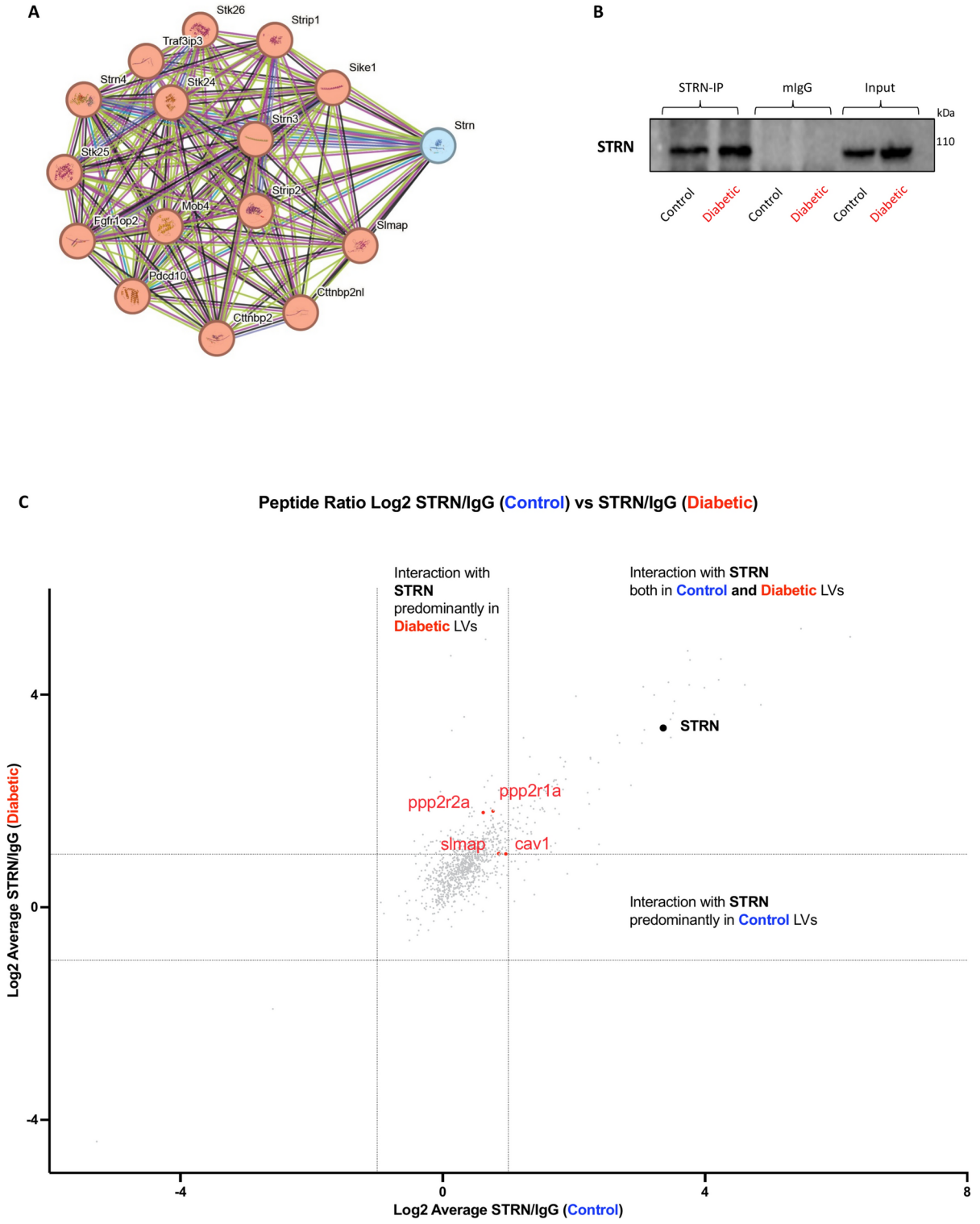

Fig. 4. Analysis of STRN interactors in control and diabetic rat left ventricle. (**A**) STRN network computed from STRING. (**B**) Immunoprecipitation (IP) with anti-STRN antibody or mouse IgG (mIgG) of total proteins from control and diabetic left ventricle of rat hearts. The STRN bands are shown using Western blot and anti-STRN antibody on the immunoprecipitated protein complex. (**C**) Scatter plot showing the interaction levels of various proteins with STRN in control, diabetic, and simultaneously both LVs. Each point on the scatter plot corresponds to a specific protein, with its position indicating the level of interaction under each condition. Ppp2r1a, ppp2r2a, slmap and cav1 are annotated to show their interactions with STRN in the diabetic LVs.

a role for STRN in protein synthesis. Mitochondrial proteins, including Hsp90b1, Tomm22, and Mavs and RNA binding and processing proteins such as Fus, PPIA, and RBBP7 were observed, along with signalling and regulatory proteins like Ywhae, Rhoa, and Rack1.

In control LV, among 11 interactors with STRN, we found several RNA binding and processing proteins, including Hnrnph1, Srsf5 and Fubp1, highlighting a potential involvement in mRNA regulation. Mitochondrial proteins including Ech1 and Mrpl2, were also prominent, suggesting a link to mitochondrial function. Additionally, kinases like Aurkaip1 and Prkaa1, as well as cytoskeletal components like Dnah12, were identified, indicating diverse biological processes associated with STRN.

Detailed annotations of all identified proteins are provided in Supplementary Table 1.

STRN interactors dynamics in diabetic left ventricle

To explore the functional annotation of STRN in diabetic hearts we investigated the STRN interactors in diabetic LV. We performed a STRING analysis to draw the PPI network of STRN in control LVs together with those complexing with STRN at both control/diabetic settings (Fig. 5A) compared to the STRN protein network in the diabetic LV only (Fig. 5B) (www.string-db.org). The analysis in Fig. 5A identified a cluster of 30 proteins interacting with STRN in control and control/diabetic LVs, and in Fig. 5B a cluster of 71 proteins interacting with STRN in diabetic LV only, including direct interactors (SLMAP, Cav-1, PPP2R1A and PPP2R2A) together with additional associated proteins.

Next, we performed functional enrichment and gene ontology (GO) analysis on these STRN interactors (Fig. 6), while focusing on the 10 most significant pathways with unique functions. The biological processes identified include actin-myosin filament sliding, mitochondrial ATP transmembrane transport, positive regulation of ER-associated ubiquitin-dependent protein catabolic process, actin filament fragmentation, regulation of voltage-gated sodium channel activity, regulation of mitochondrial membrane permeability involved in the apoptotic process, cellular response to angiotensin, mitochondrial transport, heart process, and striated muscle contraction.

The identified molecular functions cover pathways involved in cellular energetics, cytoskeletal organization and receptor-mediated signaling. These include ATP antiporter activity, voltage-gated anion channel activity, microfilament motor activity, MHC class I protein binding, structural constituent of cytoskeleton, GTP binding, GTPase activity, adenyl nucleotide binding, ATP binding, and signaling receptor binding.

Detailed analysis revealed that the reported interactors with STRN in diabetic LV are involved in specific cellular functions. These components include Myosin II filament, mitochondrial permeability transition pore complex, Myosin II complex, Myosin filament, endoplasmic reticulum (ER) chaperone complex, protein phosphatase type 2A complex, mitochondrial nucleoid, ER-Golgi intermediate compartment, microtubule, actin cytoskeleton, and cell–cell junction. The identified proteins localize to various anatomical sites within the cardiovascular and skeletal systems, including the left atrium, right atrium, left ventricle, right ventricle, blood vessels, heart, cardiovascular system, skeletal system, and muscle.

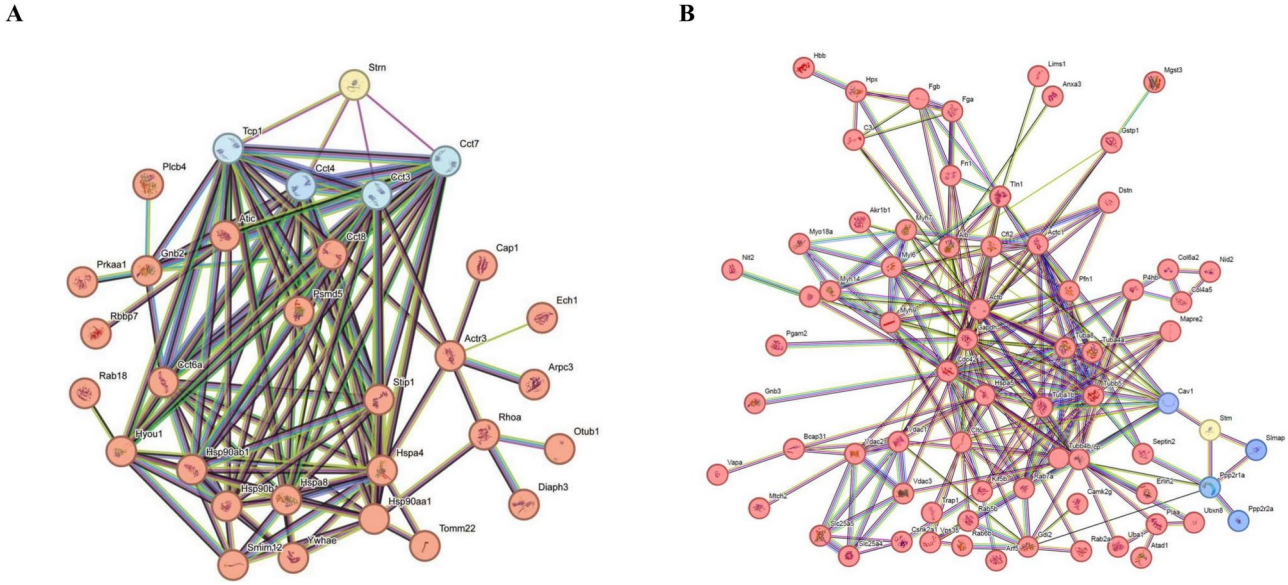

Fig. 5. STRING analysis network for STRN and its interactors in diabetic and control left ventricle. The networks show proteins interacting with STRN, with nodes representing proteins and edges corresponding to protein–protein interactions. (**A**) STRN interactors in control and both control/diabetic LV. (**B**) STRN interactors in diabetic LV.

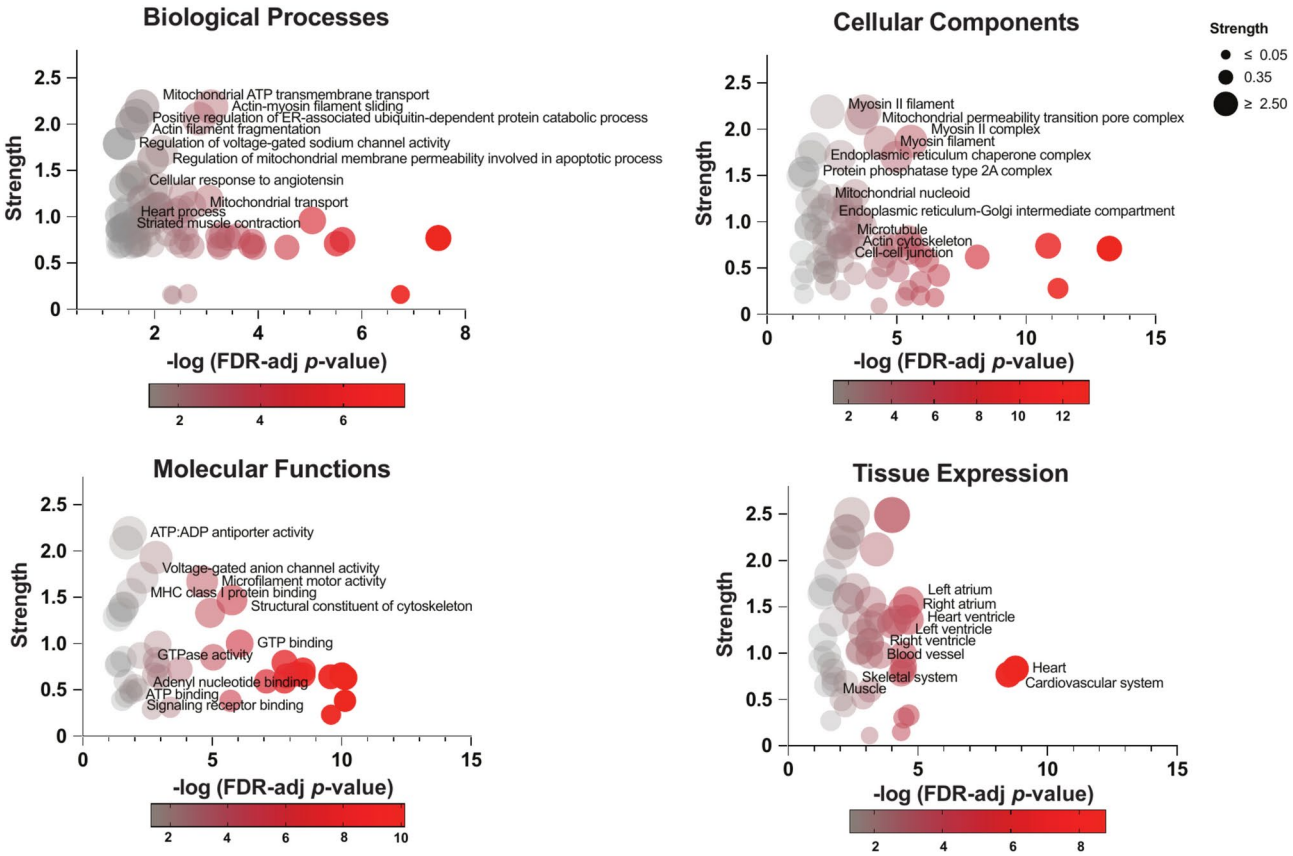

Fig. 6. Enrichment analysis of proteins interacting with STRN in diabetic left ventricle. Gene ontology categorized by biological processes, cellular components, molecular functions, and tissue expression. Statistical significance of pathway enrichment is determined using strength (bubble size) and -log (FDR-adj *p* value) (shades of red).

Cardiac STRN interacts with SLMAP in control and diabetic hearts

We sought to confirm the interactions between STRN and the regulator of cardiac function, SLMAP, that was highlighted by the proteomics analysis. Therefore, we performed IP of cardiac lysates from control and diabetic rats using a monoclonal antibody specific to SLMAP (the proteomics data being done using anti-STRN antibody), followed by Western blot analysis with either anti-STRN or anti-SLMAP (Fig. 7). Immunoblotting with anti-SLMAP showed the endogenous isoforms of SLMAP around 35, 63, and 83 kDa in the two input lanes (Control and diabetic hearts). These three isoforms, along with other isoforms of SLMAP were enriched in the IP lanes (Control and Diabetic). The presence of several protein bands of SLMAP interacting with STRN reflects a clustering of different SLMAP polypeptides in the heart (up to 26 different splice variants)[27,28]. This is in accord with our previously reported data in transgenic mice overexpressing SLMAP in the heart[29]. The absence of these bands in the IgG lanes confirms a specific and successful IP of the SLMAP isoforms. Using the anti-STRN antibody, bands were revealed in the IP and input lanes only (110 kDa), thus confirming the interaction between SLMAP and STRN in both control and diabetic hearts.

Discussion

In the present work, we employed a quantitative proteomic approach to comprehensively illustrate the proteomic landscape of STRN interactors in the diabetic LV. Our findings show that STRN expression paralleled that of ANF in the heart chambers, suggesting a potential functional link between them in cardiac remodeling. In support to this contention, recent literature highlights a correlation between STRN and key cardiac remodeling markers, including β-MHC (*Myh7*) and ANF (*Nppa*). Deletion of STRN significantly attenuated the upregulation of *Myh7* expression in response to angiotensin II treatment, suggesting a diminished hypertrophic response. Similarly, while *Nppa* expression in $STRN^{+/-}$ mice did not reach statistical significance, a trend toward reduced expression was observed, indicating a potential modulatory effect of STRN on ANF levels during cardiac stress[23]. However, this modulation may reflect STRN's involvement in a broader network influencing hypertrophy, with additional factors, such as compensatory pathways, likely contributing to ANF regulation.

Our experiments have demonstrated STRN's interaction with SLMAP, Cav-1 and PP2A-α as first line interactors based on the STRING analysis. Our findings are in line with previous studies showing that SLMAP is part of the STRN interacting phosphatase and kinase complex (STRIPAK), and that STRN co-immunoprecipitates with Cav-1[9,30]. STRN also associates with PP2A subunits[4], and variants in ppp2r1a can alter

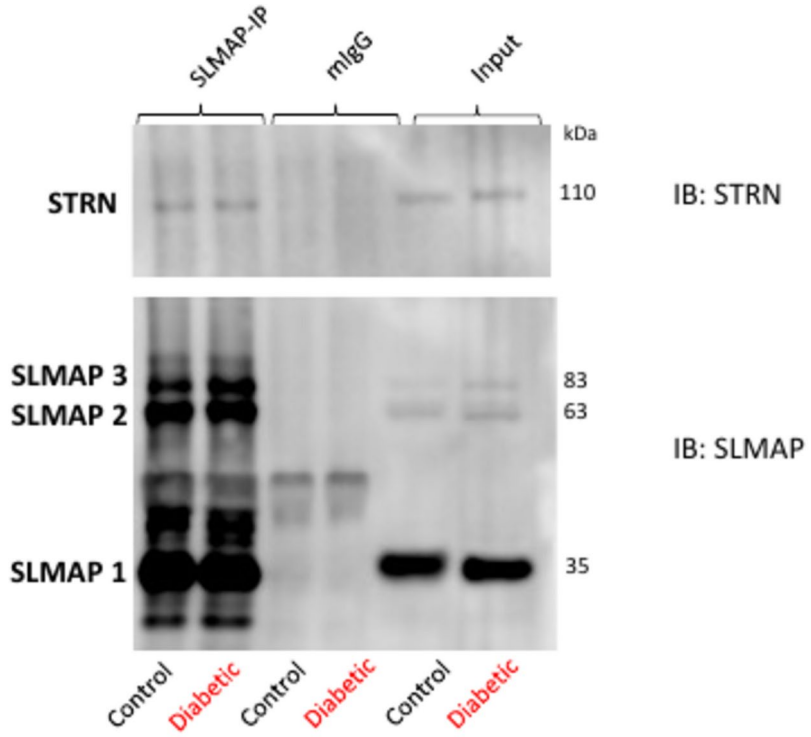

Fig. 7. Molecular interaction of STRN with SLMAP in control and diabetic heart. Immunoprecipitation (IP) with anti-SLMAP antibody or mIgG of total proteins from control and diabetic left ventricles of rat hearts. Immunoblotting (IB) with anti-STRN and anti-SLMAP. The several protein bands shown in the IP lanes using the SLMAP antibody are SLMAP polypeptides that interact together in cardiac tissues.

its interaction with STRN, thus impacting PP2A holoenzyme assembly and function[31]. Notably, our results have shown that these interactions are enhanced in diabetes, plausibly contributing to the pathological remodeling of the diabetic heart. In fact, these proteins are known for their contribution to pathological cardiac remodeling and injuries[32–34]. Given that our diabetic hearts also exhibited similar remodeling patterns, it is possible that the enhanced interactions between these proteins and STRN potentiated their signaling in the injured heart. Supporting this, previous proteomics analysis showed that SLMAP is downregulated in GLP-1RA treated mice. GLP-1RA regulated SLMAP via miR-29b-3p, and inhibiting GLP-1R reversed these effects, indicating a potential role for SLMAP in DbCM pathogenesis[35]. Meanwhile, activation of PP2A catalytic subunit has been reported to attenuate myocardial apoptosis in diabetic mice, suggesting a protective role of PP2A against cardiac remodeling in DbCM[12]. Similarly, Cav-1 knockout mice exhibited significant insulin resistance[36] and impaired cardiac function[37].

Interestingly, our GO analysis further demonstrated that these interacting proteins are involved in vital processes/signaling pathways related to diabetes pathogenesis, and are distributed across all heart chambers and the cardiovascular system. Enriched contractile functions within the protein cluster suggest that STRN and its interactors are central for cardiac contractility in diabetic heart. This could be primarily achieved by regulating the activity of voltage-gated sodium channels, striated muscle contraction, actin-myosin filament sliding, and the cellular response to angiotensin. In fact, we have previously reported that the SLMAP/STRN complex is positioned to regulate the excitation–contraction coupling in the heart[17] by impacting the sarcoplasmic reticulum structure and the expression/function of the sarcoplasmic reticulum Ca^{2+}- handling proteins[29]. We believe that the enhanced interaction of STRN with the highlighted key proteins may stabilize this complex in DbCM and could possibly lead to the pathological cardiac remodeling observed in this condition.

STRN knockout induces a gain of function of I_{Na} and impaired Ca^{2+} handling in mESC-derived cardiomyocytes, which mirrors key mechanisms underlying pathological remodeling in DbCM[24]. The gain of function of I_{Na} can lead to prolonged action potentials and increased intracellular sodium, disrupting Ca^{2+} homeostasis through sodium-calcium exchanger dysregulation[38,39]. Impaired Ca^{2+} handling further exacerbates contractile dysfunction and promotes maladaptive signaling pathways, contributing to the structural and functional deterioration characteristic of DbCM[40,41]. This highlights the critical role of STRN in influencing ion channel and Ca^{2+} handling abnormalities in the progression of diabetic heart disease.

We previously showed that cardiac STRN is expressed in cardiomyocytes and it interacts with CaM and Cav-3 in a Ca^{2+}-sensitive manner to control cardiomyocyte contraction[17]. Dysregulation of these interactions, as observed in DbCM, can impair Ca^{2+}-handling, leading to contractile dysfunction, oxidative stress, and maladaptive remodeling[3]. Similarly, the cellular response to angiotensin II has been linked to cardiac contractility through multiple mechanisms involving Ca^{2+} handling[42]. Disruptions in intracellular Ca^{2+} homeostasis

contribute significantly to impaired mechanical function in the diabetic heart, increasing the prevalence of contractile dysfunction[43]. Notably, cardiac angiotensin II has been shown to play a role in the pathophysiology of DbCM[44]. Recently, STRN's implication in angiotensin II-induced cardiac hypertrophy was highlighted[23]. Collectively, our results align with other studies showing that STRN and its interactors could contribute to pathological remodeling of the diabetic heart and cardiac dysfunction.

On the other hand, the association of Cav-1 with STRN may have relevance to STRN's role in cardiac contraction. Cardiac-specific overexpression of Cav-1 has been shown to attenuate ventricular arrhythmia, improve Ca^{2+} cycling, and reduce cardiac remodeling[45]. Cav-1 deficiency in diabetic mice led to more severe cardiac injury, increased activation of the NF-κB signaling pathway, and upregulation of genes related to hypertrophy and inflammatory fibrosis. Conversely, overexpression of Cav-1 mitigated these adverse effects, suggesting its protective role against cardiac remodeling in DbCM[15].

In addition, it was reported that an increased expression of STRN in the vasculature accounts for the activation of mineralocorticoid receptor (MR), and that STRN may regulate endocrine mechanisms in $STRN^{+/-}$ mice, through aldosterone[46,47]. These highlight a possible endocrinological role for STRN accounting for metabolic disorders, namely DbCM. Elevated MR activity promotes oxidative stress, inflammation, and fibrosis, processes that are further exacerbated by increased STRN levels, thus leading to maladaptive cardiac remodeling and impaired function[48]. These mechanisms highlight the critical interplay between MR activation, STRN, and the progression of DbCM, offering potential therapeutic targets for intervention.

Additionally, our data indicate that the cardiac STRN interactome in diabetic LV carries functional signatures mainly implicated in metabolic and cell death pathways (i.e. mitochondrial ATP transmembrane transport, mitochondrial membrane permeability in apoptotic process, ATP binding and other mitochondrial and oxidative processes). Mitochondrial functions such as ATP production, reactive oxygen species (ROS) generation and apoptosis are commonly altered in diabetes[49]. Abnormal mitochondrial Ca^{2+} handling is central to diabetic cardiac dysfunction[50]. The STRIPAK complex regulates mitochondrial function and overall cellular homeostasis, with components like mammalian STE20-like kinase 4 (Mst4) and STRN playing roles in apoptosis of cardiac cells[5,17]. STRN dynamics and its subcellular shuttling during apoptosis, along with its caspase-dependent cleavage, have been reported[51]. A novel STRIPAK assembly comprising SG2NA and DJ1 (a sensor for oxidative stress) protects against oxidative stress[52]. STRIPAK's contribution to mitochondrial function underscores STRN interactome's role in mitochondrial processes within diabetes[53,54]. ER stress is closely linked to diabetes pathogenesis, it is triggered by factors such as lipotoxicity, ROS, inflammation, and misfolded protein accumulation. This cascade not only promotes cell autophagy through a Ca^{2+}-dependent pathway but also drives apoptosis, thus significantly contributing to cardiomyocyte loss[55]. Such cellular disruptions are critical in the pathogenesis of DbCM, where heightened ER stress and apoptosis exacerbate myocardial dysfunction, leading to impaired cardiac contractility and diastolic dysfunction[56].

In conclusion, our data clearly show that the STRN interactors are remodeled in the diabetic LV, with enhanced interaction with Cav-1, SLMAP, and PP2A in this condition. Nonetheless, the expression of STRN paralleled that of the remodeling biomarker, ANF, in all four chambers of the heart: this is an additional indication of pathological signaling of STRN in the diabetic heart. Notably, the interaction between STRN and SLMAP was further validated by western blot analysis (Fig. 8). Given their functional role in diabetes-induced cardiac injuries, the retention of these above-mentioned proteins within the STRN interactome in diabetic heart suggests an operative signature in the pathogenesis of DbCM. How STRN relays signaling cascade within the heart remains elusive and calls for deeper investigations. In fact, whether this remodeling is controlled by STRN alone, its interacting proteins individually, or as an interplay between all the constituents of this signalosome remains to be determined. Thus, it is important to expand these findings to human cardiac tissue to assess therapeutic targets within the STRN interactome and explore their potential in clinical applications in DbCM.

Limitations

One limitation of our study is the use of a T1D model instead of T2D. While T1D and T2D are known to have distinct etiologies, recent studies have shown that both types share overlapping genetic and biological pathways relevant to DbCM. However, T2D specific factors including lipid dysregulation and chronic inflammation, may uniquely modulate these pathways, potentially altering STRN interactome differently. Future studies employing T2D models could help elucidate these potential differences in cardiac remodeling. Another limitation is the fact that the IP was done using an antibody against STRN. The role of STRN in inhibiting or activating its interactors remains to be determined in the settings of diabetes. Most of the interactome studies are made by overexpressing a tagged protein in cell lines to avoid possible non-specific interaction of proteins with the antibody used for IP. However, the downside of such application is that the network of proteins identified will not reflect the real network of proteins formed in the myocardium, and more importantly in diabetic settings. It is also worth noting that the IP of STRN was performed on total protein lysates from the myocardium including different types of cells, along with cardiomyocytes. Therefore, it is imperative to characterize the STRN interactome in cardiomyocytes by employing cardiomyocyte culture in diabetic settings.

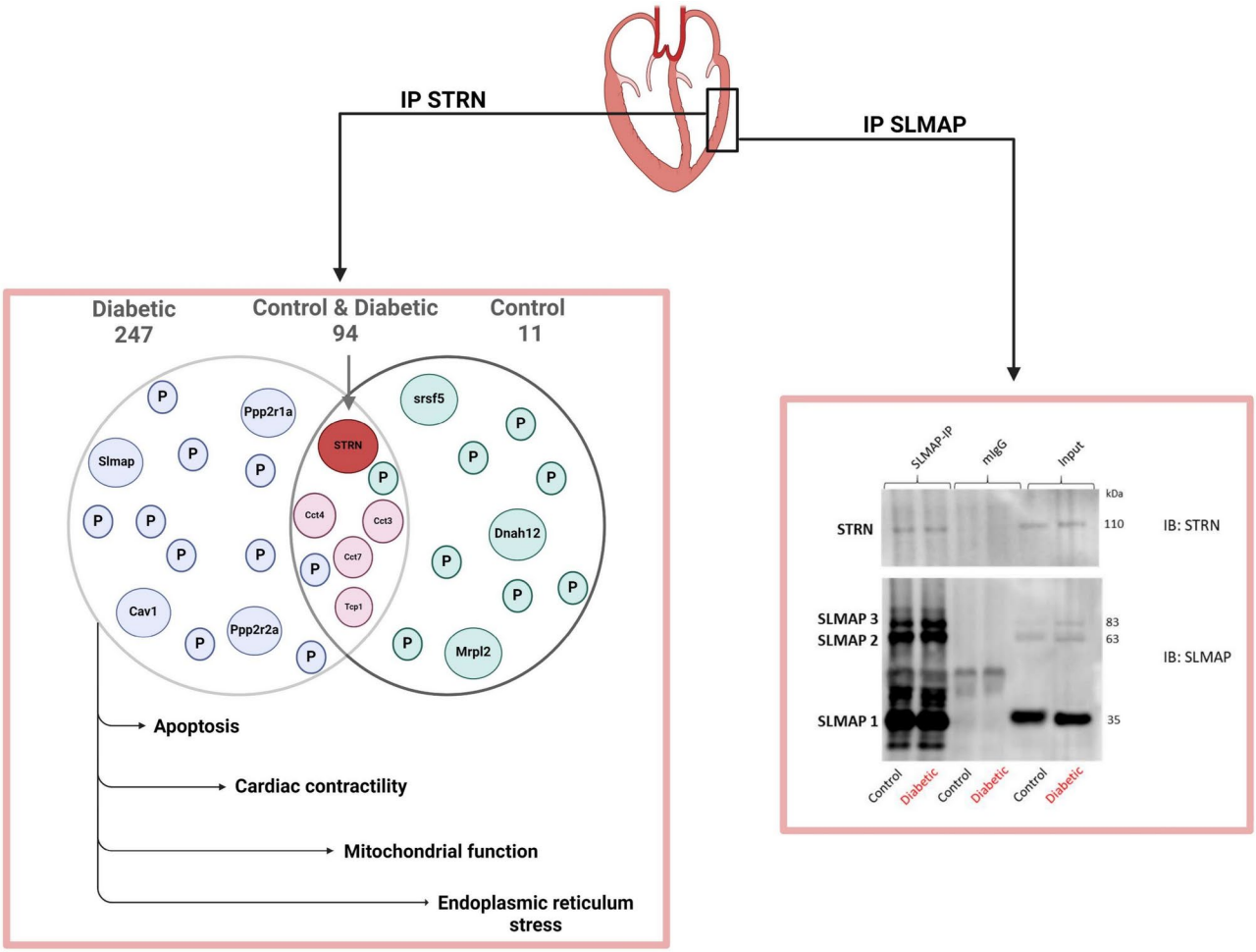

Fig. 8. STRN interactome in control and diabetic heart. The Ven diagram illustrates targeted proteins interacting with STRN in control, diabetic, and simultaneously in both LVs and shows STRN signalosome in the diabetic settings. The Western blot on the right confirms the specific interaction between STRN and SLMAP.

Data availability

The data that support the findings of this study are accessible from the corresponding author upon reasonable request.

Received: 1 August 2024; Accepted: 18 February 2025
Published online: 03 March 2025

References

1. Dillmann, W. H. Diabetic cardiomyopathy. *Circ. Res.* **124**(8), 1160–1162 (2019).
2. Global, regional, and national burden of diabetes from 1990 to 2021, with projections of prevalence to 2050: A systematic analysis for the Global Burden of Disease Study 2021. *Lancet* **402**(10397), 203–234 (2023.)
3. Jia, G., Hill, M. A. & Sowers, J. R. Diabetic cardiomyopathy: An update of mechanisms contributing to this clinical entity. *Circ. Res.* **122**(4), 624–638 (2018).
4. Moreno, C. S. et al. WD40 repeat proteins striatin and S/G2 nuclear autoantigen are members of a novel family of calmodulin-binding proteins that associate with protein phosphatase 2A. *J. Biol. Chem.* **275**(8), 5257–5263 (2000).
5. Eden, M. et al. Mst4, a novel cardiac STRIPAK complex–associated kinase, regulates cardiomyocyte growth and survival and is upregulated in human cardiomyopathy. *J. Biol. Chem.* **300**(5), 107255 (2024).
6. Li, A. X. et al. Cellular impacts of striatins and the STRIPAK complex and their roles in the development and metastasis in clinical cancers (review). *Cancers (Basel)* **16**(1), 76 (2023).
7. Bartoli, M., Monneron, A. & Ladant, D. Interaction of calmodulin with striatin, a WD-repeat protein present in neuronal dendritic spines. *J. Biol. Chem.* **273**(35), 22248–22253 (1998).
8. Gordon, J. et al. Protein phosphatase 2a (PP2A) binds within the oligomerization domain of striatin and regulates the phosphorylation and activation of the mammalian Ste20-Like kinase Mst3. *BMC Biochem.* **12**, 1–18 (2011).
9. Gaillard, S. et al. Striatin, a calmodulin-dependent scaffolding protein, directly binds caveolin-1. *FEBS Lett.* **508**(1), 49–52 (2001).
10. Nader, M. et al. SLMAP-3 is downregulated in human dilated ventricles and its overexpression promotes cardiomyocyte response to adrenergic stimuli by increasing intracellular calcium. *Can. J. Physiol. Pharmacol.* **97**(7), 623–630 (2019).

11. Ren, X. M. et al. Atorvastatin alleviates experimental diabetic cardiomyopathy by regulating the GSK-3β-PP2Ac-NF-κB signaling axis. *PLoS ONE* **11**(11), e0166740 (2016).
12. Zuo, G. F. et al. Activation of the PP2A catalytic subunit by ivabradine attenuates the development of diabetic cardiomyopathy. *J. Mol. Cell Cardiol.* **130**, 170–183 (2019).
13. Guan, Y. et al. Effects of PP2A/Nrf2 on experimental diabetes mellitus-related cardiomyopathy by regulation of autophagy and apoptosis through ROS dependent pathway. *Cell Signal.* **62**, 109339 (2019).
14. Galbo, T. et al. PP2A inhibition results in hepatic insulin resistance despite Akt2 activation. *Aging (Albany NY)* **5**(10), 770–781 (2013).
15. Gong, W. et al. Cardioprotective and anti-inflammatory effects of Caveolin 1 in experimental diabetic cardiomyopathy. *Clin. Sci. (Lond.)* **137**(6), 511–525 (2023).
16. Guo, P. et al. CAV3 alleviates diabetic cardiomyopathy via inhibiting NDUFA10-mediated mitochondrial dysfunction. *J. Transl. Med.* **22**(1), 390 (2024).
17. Nader, M. The SLMAP/Striatin complex: An emerging regulator of normal and abnormal cardiac excitation-contraction coupling. *Eur. J. Pharmacol.* **858**, 172491 (2019).
18. Al Kury, L. et al. Calcium signaling in the ventricular myocardium of the Goto-Kakizaki Type 2 diabetic rat. *J. Diabetes Res.* **2018**, 2974304 (2018).
19. Nader, M. et al. Cardiac striatin interacts with caveolin-3 and calmodulin in a calcium sensitive manner and regulates cardiomyocyte spontaneous contraction rate. *Can. J. Physiol. Pharmacol.* **95**(10), 1306–1312 (2017).
20. Meurs, K. M. et al. Genome-wide association identifies a deletion in the 3′ untranslated region of striatin in a canine model of arrhythmogenic right ventricular cardiomyopathy. *Human Genet.* **128**, 315–324 (2010).
21. Gupta, T. et al. Striatin gene polymorphic variants are associated with salt sensitive blood pressure in normotensives and hypertensives. *Am. J. Hypertension* **31**(1), 124–131 (2018).
22. Garza, A. E. et al. Variants in striatin gene are associated with salt-sensitive blood pressure in mice and humans. *Hypertension* **65**(1), 211–217 (2015).
23. Cull, J. J. et al. Striatin plays a major role in angiotensin II-induced cardiomyocyte and cardiac hypertrophy in mice in vivo. *Clin. Sci. (Lond.)* **138**(10), 573–597 (2024).
24. Benzoni, P. et al. Striatin knock out induces a gain of function of INa and impaired Ca^{2+} handling in mESC-derived cardiomyocytes. *Acta Physiologica* **24**, e14160 (2024).
25. Pang, Z. et al. MetaboAnalyst 5.0: Narrowing the gap between raw spectra and functional insights. *Nucl. Acids Res.* **49**(W1), W388–W396 (2021).
26. Dillmann, W. H. Diabetes mellitus induces changes in cardiac myosin of the rat. *Diabetes* **29**(7), 579–582 (1980).
27. Wielowieyski, P. A. et al. Alternative splicing, expression, and genomic structure of the 3' region of the gene encoding the sarcolemmal-associated proteins (SLAPs) defines a novel class of coiled-coil tail-anchored membrane proteins. *J. Biol. Chem.* **275**(49), 38474–38481 (2000).
28. Wigle, J. T. et al. Molecular cloning, expression, and chromosomal assignment of sarcolemmal-associated proteins. A family of acidic amphipathic alpha-helical proteins associated with the membrane. *J. Biol. Chem.* **272**(51), 32384–32394 (1997).
29. Nader, M. et al. Tail-anchored membrane protein SLMAP is a novel regulator of cardiac function at the sarcoplasmic reticulum. *Am. J. Physiol. Heart Circ. Physiol.* **302**(5), H1138–H1145 (2012).
30. Kück, U., Beier, A. M. & Teichert, I. The composition and function of the striatin-interacting phosphatases and kinases (STRIPAK) complex in fungi. *Fungal Genet. Biol.* **90**, 31–38 (2016).
31. Haesen, D. et al. Recurrent PPP2R1A mutations in uterine cancer act through a dominant-negative mechanism to promote malignant cell growth. *Cancer Res.* **76**(19), 5719–5731 (2016).
32. Lubbers, E. R. & Mohler, P. J. Roles and regulation of protein phosphatase 2A (PP2A) in the heart. *J. Mol. Cell Cardiol.* **101**, 127–133 (2016).
33. Gratton, J.-P., Bernatchez, P. & Sessa, W. C. Caveolae and caveolins in the cardiovascular system. *Circul. Res.* **94**(11), 1408–1417 (2004).
34. Mlynarova, J. et al. SLMAP3 isoform modulates cardiac gene expression and function. *PLoS ONE* **14**(4), e0214669 (2019).
35. Fang, P. et al. Glucagon-like peptide-1 receptor agonist protects against diabetic cardiomyopathy by modulating microRNA-29b-3p/SLMAP. *Drug Des. Devel. Ther.* **17**, 791–806 (2023).
36. Gonzalez-Munoz, E. et al. Caveolin-1 loss of function accelerates glucose transporter 4 and insulin receptor degradation in 3T3-L1 adipocytes. *Endocrinology* **150**(8), 3493–3502 (2009).
37. Jasmin, J.-F. et al. Caveolin-1 deficiency exacerbates cardiac dysfunction and reduces survival in mice with myocardial infarction. *Am. J. Physiol.-Heart Circul. Physiol.* **300**(4), H1274–H1281 (2011).
38. Liu, T., et al. Altered calcium handling produces reentry-promoting action potential alternans in atrial fibrillation-remodeled hearts. JCI Insight, 2020. **5**(8).
39. Despa, S. Myocyte [Na+] i dysregulation in heart failure and diabetic cardiomyopathy. *Front. Physiol.* **9**, 1303 (2018).
40. Tse, G. et al. Cardiac dynamics: alternans and arrhythmogenesis. *J. Arrhythmia* **32**(5), 411–417 (2016).
41. Pereira, L. et al. Calcium signaling in diabetic cardiomyocytes. *Cell Calcium* **56**(5), 372–380 (2014).
42. Zhang, M. et al. Contractile function during angiotensin-II activation: Increased Nox2 activity modulates cardiac calcium handling via phospholamban phosphorylation. *J. Am. Coll. Cardiol.* **66**(3), 261–272 (2015).
43. Singh, R. M. et al. Hyperglycemia-induced cardiac contractile dysfunction in the diabetic heart. *Heart Fail. Rev.* **23**(1), 37–54 (2018).
44. Zhou, G. et al. Metallothionein suppresses angiotensin II-induced nicotinamide adenine dinucleotide phosphate oxidase activation, nitrosative stress, apoptosis, and pathological remodeling in the diabetic heart. *J. Am. Coll. Cardiol.* **52**(8), 655–666 (2008).
45. Wu, S.-J. et al. Cardiac-specific overexpression of caveolin-1 in rats with ischemic cardiomyopathy improves arrhythmogenicity and cardiac remodelling. *Can. J. Cardiol.* **39**(1), 73–86 (2023).
46. Pojoga, L. H. et al. Activation of the mineralocorticoid receptor increases striatin levels. *Am. J. Hypertens.* **25**(2), 243–249 (2012).
47. Gromotowicz-Poplawska, A. et al. Enhanced thrombotic responses are associated with striatin deficiency and aldosterone. *J. Am. Heart Assoc.* **10**(22), e022975 (2021).
48. Brown, N. J. Contribution of aldosterone to cardiovascular and renal inflammation and fibrosis. *Nat. Rev. Nephrol.* **9**(8), 459–469 (2013).
49. Rolo, A. P. & Palmeira, C. M. Diabetes and mitochondrial function: Role of hyperglycemia and oxidative stress. *Toxicol. Appl. Pharmacol.* **212**(2), 167–178 (2006).
50. Diaz-Juarez, J., et al., Mitochondrial calcium handling and heart disease in diabetes mellitus. Biochimica et Biophysica Acta (BBA)-Molecular Basis of Disease, 2021. **1867**(1): p. 165984.
51. Nader, M. et al. Striatin translocates to the cytosol of apoptotic cells and is proteolytically cleaved in a caspase 3-dependent manner. *Heliyon* **6**(9), e04990 (2020).
52. Bisoyi, P. et al. In the rat midbrain, SG2NA and DJ-1 have common interactome, including mitochondrial electron transporters that are comodulated under oxidative stress. *Cell. Mol. Neurobiol.* **43**(7), 3061–3080 (2023).
53. Jain, B. P. et al. SG2NA is a regulator of endoplasmic reticulum (ER) homeostasis as its depletion leads to ER stress. *Cell Stress Chaperones* **22**(6), 853–866 (2017).
54. Back, S. H. & Kaufman, R. J. Endoplasmic reticulum stress and type 2 diabetes. *Annu. Rev. Biochem.* **81**, 767–793 (2012).

55. Yang, L., et al., *Endoplasmic reticulum stress and protein quality control in diabetic cardiomyopathy.* Biochimica et Biophysica Acta (BBA) - Molecular Basis of Disease, 2015. **1852**(2): p. 209–218.
56. Bugger, H. & Abel, E. D. Molecular mechanisms of diabetic cardiomyopathy. *Diabetologia* **57**(4), 660–671 (2014).
57. Jumper, J. et al. Highly accurate protein structure prediction with AlphaFold. *Nature* **596**(7873), 583–589 (2021).
58. Li, A. X. et al. Cellular impacts of striatins and the STRIPAK complex and their roles in the development and metastasis in clinical cancers (review). *Cancers* **16**(1), 76 (2024).

Acknowledgements

This work was supported by a grant from Khalifa University of Science and Technology to MN (Grant #FSU-2021-024).

Author contributions

S.C.: Writing—original draft, Writing—review and editing, Methodology, Investigation, Formal analysis. W.A.: Writing—original draft, Data curation, Formal analysis. C.A.H. Data curation, Formal analysis, Writing—review and editing. L.A. Formal analysis, Writing—review and editing. T.V. Investigation, Writing—review and editing. P.Z. Writing—review and editing. S.S. Writing—review and editing. F.C.H. Writing—review and editing. A.A.K. Writing—review and editing. M.N. Conceptualization, Methodology, Investigation, Visualization, Formal analysis, Supervision, Validation, Writing—review and editing.

Competing interests

The authors declare no competing interests.

Additional information

Supplementary Information The online version contains supplementary material available at https://doi.org/10.1038/s41598-025-91098-6.

Correspondence and requests for materials should be addressed to M.N.

Reprints and permissions information is available at www.nature.com/reprints.

Publisher's note Springer Nature remains neutral with regard to jurisdictional claims in published maps and institutional affiliations.